Published in final edited form as:
J Immunol. 2009 September 1; 183(5): 3177–3187. doi:10.4049/jimmunol.0804233.

Modulation of Single-Cell IgG Secretion Frequency and Rates in Human Memory B Cells by CpG DNA, CD40L, IL-21 and Cell Division[‖]

Alicia D. Henn[*,§], **Jonathan Rebhahn**[‡], **Miguel A. Brown**[*,§], **Alison J. Murphy**[*,§], **Mircea N. Coca**[*,§], **Ollivier Hyrien**[†,§], **Tina Pellegrin**[*,§], **Tim Mosmann**[‡,§,¶], and **Martin S. Zand**[*,§,¶]

[*]Division of Nephrology

[†]Department of Biostatistics and Computational Biology

[‡]Center for Vaccine Biology and Immunology

[§]Center for Biodefense Immune Modeling

[¶]Department of Microbiology and Immunology

Abstract

During the recall response by CD27+ IgG class switched human memory B cells, total IgG secreted is a function of (1) the number of IgG secreting cells (IgG-SC) and (2) the secretion rate of each cell. Here we report the quantitative ELISPOT method (qELISPOT) for simultaneous estimation of single cell IgG secretion rates and secreting cell frequencies in human B cell populations. We found that CD27+ IgM^{neg} memory B cells activated with CpG and cytokines had considerable heterogeneity in the IgG secretion rates, with two major secretion rate subpopulations. B cell receptor cross-linking reduced the frequency of cells with high per-cell IgG secretion rates, with a parallel decrease in $CD27^{hi}$ B cell blasts. Increased cell death may account for the BCR-stimulated reduction in high-rate IgG-SC $CD27^{hi}$ B cell blasts. In contrast, the addition of IL-21 to CD40L +IL-4 activated human memory B cells induced a high-rate IgG-SC population in B cells with otherwise low per-cell IgG secretion rates. The profiles of human B cell IgG secretion rates followed the same biphasic distribution and range irrespective of division class. This, along with the presence of non-IgG-producing, dividing B cells in CpG+ck-activated B memory B cell populations, is suggestive of an "On/Off switch" regulating IgG secretion. Finally, these data support a mixture model of IgG secretion in which IgG secreted over time is modulated by the frequency of IgG secreting cells and the distribution of their IgG secretion rates.

[‖]Grant Support: This work was supported by NIH grants N01-AI-50020 (A.H., O.H., J.R., T.M., M.Z.), N01-AI-50029 (T.M., M.Z.) and R01 AI069351 (M.Z., O.H., M.C.).

Corresponding Author: Martin S. Zand, MD, PhD Professor of Medicine University of Rochester Medical Center 601 Elmwood Ave – Box 675 Rochester, NY 14642 Vox: 585.275.4517 Fax: 585.486.1043 Martin_Zand@urmc.rochester.edu.

Author Contributions – A.D.H. designed the bead standards, performed experiments, analyzed data and wrote the paper J.R., T.M. and M.B. designed the image analysis system. M.C., A.M., and T.P. performed experiments, analyzed data, and made the figures for the manuscript. O.H. performed statistical analyses. M.Z. directed the experimental design and implementation, analyzed data, and wrote the paper.

Competing Interests Statement – The authors declare that they have no competing financial interests.

Keywords

Memory B cells; Immunoglobulin; ELISPOT; antibody secretion

Introduction

During the recall response of class switched IgG^+ $CD27^+$ memory B cells, the total amount of immunoglobulin (IgG) secreted during an *in vitro* assay is a function of the total number of living cells (PB_{live}), the fraction of these cells secreting IgG (φ_{ASC}), the rate at which IgG is secreted by each cell (σ_{IgG}), and the duration of the assay. This can be described quantitatively by the equation in Figure 1a. Antibody secreting cells (ASC) are a fraction of the total number of live and dividing B cells. The number of ASC increases after activation by both cell division and differentiation of non-secreting B cell blasts into IgG ASC, resulting in an increase in IgG released (1). We do not know, however, whether the total amount of IgG secreted during a recall response results from a division-linked increase in the IgG secretion rate of each cell (σ_{IgG}) with each new generation of cells or if σ_{IgG} is simply fixed for all activated B cells. In this report we investigate this question by directly measuring the frequency of IgG secreting cells and rate of IgG secretion for each individual cell (σ_{IgG}) within multiple populations of CD27+ IgG+ memory B cells activated with CpG and cytokines (CpG+CK).

CD27+ memory B cells activated by CpG_{2006} oligodeoxynucleotides (CpG) via TLR-9 signaling (2) respond by rapid proliferation, differentiation into plasmablasts, and an increase in Ig secretion (3,4). We tested three hypotheses (Fig. 1) designed to describe the kinetics by which individual $CD27^+$ IgG class switched memory B cells activated by CpG DNA in the presence of exogenous IL-2, IL-10, and IL-15 (CpG+CK) secrete IgG. In the secretory rate maturation hypothesis, memory B cells divide and differentiate, with σ_{IgG} increasing with each cell division until a maximum rate is reached. This mechanism seems plausible as IgG secreting B cell blasts, plasma cells and hybridoma clones exhibit heterogeneity of IgG secretion rates (5-8). A competing hypothesis is that antibody secretion is controlled by a stochastic binary "On/Off" switch, in which all B cells secreting IgG do so at a rate (σ_{IgG}) which is fixed irrespective of the number of post-activation cell divisions or other factors (9,10). In this second hypothesis, memory B cell activation results in memory B cell proliferation (B cell blasts), and some of these B cell blasts "switch on" where IgG is secreted by each cell in this population at individual rates that conform to a fixed statistical distribution. A third hypothesis would allow for multiple subpopulations of IgG secreting B cell blasts, and within each of these populations antibody secretion is switched "on/off" with a fixed IgG secretion rate distribution characteristic of each population. In this last model, there is a mixture of different B cell subpopulations with high or low Ig secretion rates (σ_{IgG}) with each responding to environmental stimuli by selective proliferation, death or differentiation. The differential responses of each sub-population would provide a mechanism for fine tuning the amount of IgG secreted by the overall population based on environmental context and cues, such as cytokines or costimulatory signals.

The fraction of antibody secreting cells (φ_{ASC}) in a population can be measured by conventional ELISPOT but this method provides little quantitative information about variations in σ_{IgG} between individual antibody secreting cells (11). Because only a fraction of activated B cells actually secretes IgG in most experiments, dividing the total amount of IgG, as measured by ELISA, by the number of cells secreting IgG, gives an average σ_{IgG}, but no information

regarding the variation or range of σ_{IgG} among individual cells a population of B cell blasts or plasma cells.

In this manuscript, we describe a quantitative ELISPOT method (qELISPOT) that permits measurement of IgG secretion rates for each individual cell, and the frequency of IgG secreting cells within the same experimental population. The standard ELISPOT method can enumerate immunoglobulin secreting B cells within an activated population (11). Intuitively, spot size and optical density should correlate with the total amount of immunoglobulin secreted over the time a cell is in contact with the ELISPOT membrane. With image analysis software it is possible to both count individual spots, and to quantify the total spot area and the spot intensity (12). Total spot intensity is sum of the spot pixel values within the spot area, expressed in this manuscript in arbitrary pixel intensity units (Int-U). The quantitative relationship between spot intensity and the IgG secretion rate σ_{IgG} (fg IgG•hour^{-1}•cell^{-1}) can be estimated by releasing defined quantities of IgG from polymer beads of varying surface area and binding capacity in parallel ELISA and ELISPOT assays. Each bead type creates a distribution of spots with a relatively uniform area and intensity distribution, and the parallel ELISA allows measurement of total IgG released for a known number of beads. The result can be used to correlate spot intensity to femtograms of IgG.

We coupled the quantitative ELISPOT (qELISPOT) method with CFSE cell kinetic analysis to measure the contribution of cell division to total IgG secreted, σ_{IgG} , and φ_{ASC}. The combined methods were then used to study the effect of different stimulation conditions on the distribution of single cell antibody secretion rates of CD27+ IgM^{neg} memory B cells by division number, and to discriminate between the hypotheses of IgG production: (1) secretion rate maturation, in which IgG secretion rates increase with post-activation division class and (2) “On/Off” secretion, in which σ_{IgG} are fixed for each ASC within a range, and are turned on or off by external signals, and (3) the mixture model, where sub-populations of φ_{ASC} have different statistical distributions of IgG secretion rates (σ_{IgG}).

Materials and Methods

Human Subjects Protection

This study was approved by the Research Subjects Review Board at the University of Rochester Medical Center. Informed consent was obtained from all participants. Research data were coded such that subjects could not be identified, directly or through linked identifiers, in compliance with the Department of Health and Human Services Regulations for the Protection of Human Subjects (45 CFR 46.101(b)(4)).

Myeloma Cell Culture

IgG-secreting myeloma cells, MPR-1130 (established in our laboratory), MC/CAR and Ramos cell lines (ATCC, Manassas, VA) were maintained in log-phase growth as previously described (13).

Antibody Reagents

For ELISPOT and ELISA capture Ab, we used Mouse anti-Human IgG (H+L) (Jackson, West Grove, PA). For ELISPOT detection, we used phosphatase-conjugated Goat anti-Human IgG (Jackson, West Grove, PA), for ELISA detection, peroxidase-conjugated Goat anti-Human IgG and peroxidase-conjugated bovine anti-goat IgG, standard curves made with human IgG F(ab)$_2$ fragment (all from Jackson, West Grove, PA). FACS analysis was performed using the following; Anti-CD19 PECy5, anti-CD27 allophycocyanin, anti-CD38 PECy7, anti-CD38 allophycocyanin, anti-IgG FITC, anti-IgG PECY5, anti-IgM PE, anti-CD19 Biotin, isotype controls of mouse IgG1k conjugated to FITC, Pacific Blue, PE, PECy5, PECy7, Alexa 700,

allophycocyanin, and Biotin, PE (all from BD Bioscience, San Diego, CA), anti-CD20 Pacific Blue, anti-CD27 Alexa 700, (eBioscience, San Diego, CA), and Streptavidin-Qdot 705 (Invitrogen Carlsbad, CA).

B Cell Isolation

Human peripheral blood mononuclear cells were isolated by Ficoll gradient centrifugation as previously described(4). Negative magnetic immunoaffinity bead separation (Miltenyi Biotec, Auburn, CA) was used to isolate total $CD19^+$ B cells. Anti-IgM-PE antibody (BD Biosciences, San Diego, CA) and anti-PE beads (Miltenyi Biotec, Auburn, CA) were used to deplete the IgM expressing naïve and memory B cells from the CD19+ B cell population. IgA was expressed by a small fraction (2-11%) of remaining cells and this proportion did not change significantly after 72 hours of stimulation with CpG in the presence of recombinant human B cell activating factor (BAFF), IL-2, IL10, and IL-15.

Flow Cytometric Analysis

Flow cytometric analysis of B cell surface and intracellular markers and CFSE labeling was performed as previously described (4) on an LSR II cytometer with FACS Diva data acquisition software. Results were analyzed using FlowJo software (Treestar, Ashland, OR). Flowjo software (Treestar, Ashland, OR) was used to display and gate data.

B Cell Stimulation

Cells from a single donor were split into separate stimulation cultures as previously described (4). CpG 2006 (10ng/ml, Oligos, etc., Wilsonville, OR), plus recombinant human cytokines IL-2 (20 IU/ml), IL-10 (50ng/ml), IL-15 (10ng/ml) (all from BD Biosciences, San Diego, CA), and recombinant BAFF (75ng/ml, Chemicon, Temecula, CA) were used in PC-L medium (IMDM medium, lacromin (50μg/ml, Seracare, Milford, MA), insulin (5μg/ml, Sigma-Aldrich, St. Louis, MO), penicillin/streptomycin (1x, Invitrogen, Carlsbad, CA), gentamicin (15μg/ml, Invitrogen,), heat-inactivated fetal bovine serum (10% v/v, Invitrogen), normocin (0.1% v/v, Invivogen, San Diego, CA)) in round-bottomed 96-well plates (BD Biosciences, San Diego, CA). BCR-cross-linking was accomplished in some cultures using soluble $F(ab)_2$ fragments of goat anti-human IgA, IgG, and IgM (H+L) (Jackson, West Grove, PA). Before ELISA and ELISPOT assays, cells treated with BCR-crosslinking antibodies were saturated with human soluble IgG F(ab) fragments ($1mg/10^6$ cells, Jackson, West Grove, PA) and washed four times in a large volume of PBS. This step was performed to prevent inadvertent capture of IgG secreted by the cells during the assay by residual BCR-crosslinking anti-IgG on the cell surface. Some sets of cells were stimulated by co-culture with irradiated fibroblasts expressing CD40L, as previously described (15), rhuIL-4 and/or rhuIL-21 (BD Biosciences) in 48-well flat-bottomed plates(14). Flow cytometry was used to assess CD40L expression of the fibroblasts. All cells were cultured for 72hrs or 96hrs after isolation at 37°C, 5% CO_2 before being placed into assays.

Antibody Coated Paramagnetic Bead Preparation

Streptavidin-coated paramagnetic microspheres 8, 10 or 12 microns in diameter (Bangs Lab, Fishers, IN; micromod Partikeltechnologie GmbH, Germany) were incubated in DSB-IgG (Human IgG from Jackson, West Grove, PA) Invitrogen, Carlsbad, CA). Sixteen micron diameter beads (Micromod DE, Germany) were first coated with streptavidin (Sigma-Aldrich, St. Louis, MO) using (PolyLink Coupling Kit, Bangs Lab, Fishers, IN), then incubated in DSB-IgG. Additional streptavidin was attached to 10 or 16 micron beads using an 8-branch PEG polymer with amino linker groups (NOF America, White Plains, NY). All beads were washed overnight in phosphate-buffered saline (PBS) plus 2% w/v bovine serum albumin at room temp

with slow mixing on a rotator. Bead concentration was determined by manual count using a hemocytometer (VWR, Westchester, PA).

Pre-spotting ELISPOT wells with beads

Control wells of 96 well assay plates were seeded with IgG bearing beads, each bead type in triplicate wells. The IgG was released from the beads, and then the wells were washed in advance of all experiments. Three columns of each twelve-column (96-well) plate were pre-wetted with 35% ethanol for 1 min, rinsed with PBS, then coated with for 1 hr with 10μg/ml mouse anti-human IgG capture antibody (Jackson, West Grove, PA), washed three times with sterile PBS, and blocked with PBS + 2% Bovine Serum Albumin (Sigma-Aldrich, St. Louis, MO). The ferro-magnetic IgG coated beads were plated at a density of 300 beads/well and D-biotin (9mM final, Invitrogen, Carlsbad, CA) added to each well to release the low-affinity DSB-IgG from streptavidin. The ELISPOT plates were placed on large rare-earth magnets to settle the magnetic beads rapidly to the well membrane and immobilize them during antibody release. Beads were also placed into ELISA plates coated with the same capture antibody used in the ELISPOT assays. ELISPOT and ELISA plates were incubated at 37°C for 4 days and the bead-containing wells washed with PBS+ 0.1% Tween-20 (Sigma-Aldrich, St. Louis, MO), rinsed with water, and air-dried.

Paired ELISA-ELISPOT assays

ELISPOT plates pre-spotted with beads were prepared for assay by coating, washing and blocking unoccupied wells as stated above for bead pre-spotting. Matching ELISPOT and ELISA plates were plated with 9 replicate wells of beads for standard curve generation. Time point plates were plated with pre-spotted with triplicate wells of each bead standard. B cells were collected, washed, counted with trypan blue for viability to calculate live cell numbers for plating. At each time point, ELISPOT plates were washed with PBS, rinsed with distilled water, air-dried and stored overnight in the dark at room temperature before development as a batch with the standard curve ELISPOT and ELISA bead plates.

ELISA plates were processed by incubation for 1 hour at 37°C with horseradish peroxidase-conjugated goat-anti-human IgG in PBS with 2% BSA, washed, and then incubated with bovine-anti-goat IgG-HRP in PBS + 2% BSA for 1 hour at room temperature. The wells were washed and color developed using ABTS One Component Microwell Substrate (Southern Biotech, Birmingham, AL) and read at 405nm on a Benchmark Plus microplate spectrophotometer (Bio-Rad, Hercules, CA).

ELISPOT plates were processed by re-wetting well membranes for 1 minute with 35% ethanol, rinsing with PBS and incubating with detecting antibody for 2 hours at room temperature. The wells were washed with PBS plus 0.1% Tween 20 (Sigma-Aldrich, St. Louis, MO), and incubated with alkaline phosphatase substrate kit III (Vector, Burlingame, CA) for 30 minutes at room temperature in the dark. The wells were washed with tap water and air-dried. Individual ELISPOT well membranes were punched out of the plates onto adhesive film, scanned at 3600 dots per inch with a HP Scanjet 8300 high-resolution flatbed scanner (Hewlett Packard, Palo Alto, CA), set for no auto-correction, no lighten/darken, no sharpening, and no color adjustment. Each plate image was saved as a single bitmap file.

ELISPOT Analysis

Each plate bitmap image was divided into individual well images using image processing software developed in MATLAB as previously described (12). The image in each red, green, blue-channel was processed independently from the other channels. Image contrast was enhanced using a custom Laplacian filter, and noise was reduced using a 3×3 median filter applied 3 times. The image was then inverted, a watershed transform applied. The watershed

image was converted to binary. Non-uniform background was then approximated from the filtered image using the watershed image as a mask. The background was then subtracted from the filtered image, and segmented by a threshold. Final segmentation was achieved by multiplying the segmented image by the binary watershed image. Each segment, representing a spot, was then assigned a unique identification number. These segments were used for subsequent spot measurements.

Total spot intensity was calculated by:

$$I_k = \sum_{i=1}^{p_k} I_{ki}$$

which is the sum of the pixel intensity values (I_{ki}) in spot k of all the pixels from 1 to p_k within the spot boundaries. Spot circularity was calculated by:

$$C_i = \frac{\mu_R - 2\sigma_R}{\mu_R}$$

Where μ_R and σ_R are the mean and standard deviation of R, defined for any spot i:

$$R_i = \sum_{j=1}^{s} \sqrt{(x - m_{ij})^2 + (y - n_{ij})^2}$$

where s is the total number of pixels on the perimeter of the spot, (x,y) are the coordinates of the centroid of the spot, and (m_{ij}, n_{ij}) are the coordinates of the j^{th} pixel on the spot perimeter. Thus, if all the perimeter spots are equidistant from the centroid, $\sigma_R = 0$, and C=1, indicating a perfect circle.

Statistics

Descriptive statistics (mean, geometric mean, standard deviation) and regression analyses performed using Statistica (StatSoft, Tulsa, OK). Group comparisons were performed using Student's t-test and the non-parametric Wilcoxon rank sum test (16). Histogram plotting for qELISPOT population parameters was performed using Flowjo software. Comparisons of spot distributions were performed using the distribution-free two-sample Kolmogorov-Smirnov test (16).

RESULTS

CpG+CK Stimulation of memory B cells produces a biphasic IgG secretion profile

We first measured the frequency and IgG secretion rates of peripheral blood isolated human IgM^{neg} memory B cells stimulated for 72 hours with unmethylated CpG_{2006} oligodeoxynucleotide in the presence of IL-2, IL-10, IL-15 and BAFF (CpG+CK) (Fig. 2). IgG ELISPOT data was acquired with a high-resolution optical scanner and spots were analyzed as described (12). Measured spot parameters included spot area (number of pixels), intensity (the sum of pixel values of the spot), the location of each spot in the well, and spot circularity. Data were exported in Flow Cytometry Standard 3 listmode format, gated and analyzed using standard flow cytometry analysis software.

Figure 2a shows representative unprocessed IgG ELISPOT images from CpG+CK-stimulated and unstimulated B cells, and the corresponding processed images with spot boundaries delineated. A large increase in the number of IgG spots (34 spots control vs. 751 CpG+CK from 1200 total cells plated; representative of 6 separate experiments) can be seen with CpG +CK stimulation. A representative three-dimensional intensity plot of one spot is shown in Fig. 2b. The coordinates of each pixel (x, y) are used to calculate spot area. The z-axis values correspond to the pixel intensities, which are summed over the spot area to calculate the spot Intensity (Int).

Spot circularity was used to discriminate between spot artifacts and spots produced by cells (Fig. 2c). A perfectly circular spot has a value of C=1.0. Many of these artifacts have a very small area and are found at the edge of the well. If spots of C<0.6 were included, the total number of spots would routinely exceed the total number of cells plated in the experiment by a factor of 2-4. Thus, these artifacts were identified and eliminated from the analysis by creating a pooled sample from all 96 wells of each ELISPOT plate and using a bivariate plot of radial distance from the well center versus spot circularity. Note that this gating strategy also allowed us to identify and include highly circular “true” spots at the well edge in the final analysis.

After gating, data from each set of replicate wells were pooled and analyzed. The increase in number and size of spots with CpG+CK seen in the images in Fig. 2a, is reflected in Fig. 2d, spot intensity and spot area histograms (n=6 wells per sample). Histograms reveal a range of spot size and intensity distributions spanning two logs in pixel area and four logs in intensity. Total spot intensity is a multiple of the area times the amount of antibody captured in that area, so it is not surprising that intensity shows much clearer separation between high and low IgG containing spots. Two major subpopulations were seen, smaller IgG spots with intensities in the same range as spots found in cultures of unstimulated B cells (<2000 Int-U) and a second population of spots produced by cells that have increased their IgG secretion in response to CpG+CK stimulation (>2000 Int-U). Total IgG secretion of the population, as measured by ELISA, also increased in response to CpG+CK stimulation (145.1±77.5 pg/1000 cells CpG +CK, 5.27±0.53 pg/1000 cells unstimulated). We next quantified the IgG secretion rates in the two IgG-SC populations present in this biphasic response.

Mapping spot intensity values to antibody secretion

We estimated single cell IgG secretion rates using a standard curve that translated spot intensity into fg IgG•cell^{-1}• hour^{-1} incubated. We used known numbers of streptavidin coated beads of different sizes and binding capacities to release DSB-biotin-conjugated IgG in ELISA or ELISPOT assays performed at the same time with the same capture antibodies and under the same conditions. Figure 3 shows images taken from ELISPOT wells with spots produced by these beads. A standard curve was obtained by plotting mean spot intensity against IgG measured by ELISA. Figure 3 demonstrates the calculation of a standard curve, relating spot intensity to amount of IgG released per spot. Individual cell IgG secretion rates (σ_{IgG}) measured in our assays ranged from 52.2 ± 178 fg IgG•cell^{-1}•6 hour $^{-1}$ to 44,961 ± 29,145 fg IgG•cell^{-1}• 6 hour $^{-1}$ (n=15 separate experiments).

The intensity of IgG-spots generated by cells or beads is a better measure of IgG secreted than spot area

To assess which parameter best correlates with IgG released per spot, we measured the mean intensities and the mean areas of ELISPOTs made by the myeloma cell lines MC/CAR, MPR1130 (1-6 hour time-points), and IgG-releasing beads (Fig. 4). Three-dimensional spot images are also shown, demonstrating changes in spot morphology as the spots increase in size. In all cases, spot area and intensity had a monotonically increasing relationship, suggesting that either parameter could be used to relate spot size to IgG released. Under these conditions,

we did not observe complete saturation of the pixel values for the central portion of the spots (data not shown). Total spot intensity, the total of the pixel values for each spot, was directly related to the spot area, but spot intensity histograms yielded a broader range of spot values. We thus chose total spot intensity for our comparisons as it provided a clearer separation between different populations of spots.

Assay incubation time (t_{inc}) must be adjusted to stay within the standard curve range

One obvious difference between IgG-releasing beads and B cells is that while beads release a fixed amount of IgG, B cells actively synthesize IgG. Thus, both beads and spots are similar in their release of IgG over time. Although the total amount of IgG released by beads is limited by the bead surface area and fixed binding capacity, cellular IgG secretion is limited by the secretory rate. Therefore, the length of time the cells are in contact with the ELISPOT membrane in the assay plate (t_{inc}) is a critical factor in the amount of IgG captured as spots, and in reaching a saturation point of the capture molecules on the ELISPOT membrane. To better explore this issue, we examined the effect of incubation time on spot intensity using MPR1130 myeloma cells which produce very large IgG-spots and have a high mean secretion rate as determined by ELISA (492.02 ± 36.892 fg IgG•cell^{-1}• hour $^{-1}$), and MC/CAR myeloma cells that produce smaller spots, secreting IgG at a lower mean rate (30.786 ± 10.074 fg IgG•cell^{-1}• hour $^{-1}$) (Fig. 5). In these experiments, MPR spots with intensity values greater than 2×10^5 Int-U merged with neighboring spots, confounding analysis. However, the number of spots produced by low-rate IgG-secreting MC/CAR cells was still increasing at 12 hours, suggesting that more cells secreting IgG at very low rates produce detectable spots in longer incubations. These observations invited two conclusions: (1) that the spot size increases with time, so the assay sensitivity can be ‘tuned’ by varying the incubation time, and (2) spot sizes with real cells can be quite heterogeneous, such that cells producing IgG at low secretion rates may only be detected in longer assays. Thus, subsequent experiments were designed by performing initial “range-finding” pilot studies to tune the incubation time and insure that cells secreting IgG at low secretion rates were, within the limits of the method, captured in each experiment series.

B cell receptor cross-linking with soluble anti-IgG F(ab)$_2$ fragments inhibits the CpG+CK stimulated increase in IgG-SC

CD27+ memory B cells activated by CpG_{2006} oligodeoxynucleotides (CpG) via TLR-9 signaling (2) respond by rapid proliferation, differentiation into B cell blasts, and an increase in Ig secretion (3,4,17). These changes are division linked, such that the frequency of IgG secreting B cells increases with each post-activation mitosis.(1,10) Depending upon cell maturation and culture conditions, BCR activation has also been shown to enhance CpG induced proliferation in some studies (17-20) and inhibit it in others. (21) Thus, total IgG secretion by activated memory B cell populations could change due to either the percentage of cells able to secrete IgG, φ_{ASC}, or the secretion rate per cell, σ_{IgG}. Therefore, we performed the following experiments to examine the contributions of proliferation, cell death, secretory rate, and the frequency of IgG-SC to antibody production in CD27+ human memory B cells activated by CpG+CK, BCR crosslinking with soluble anti-IgG F(ab)$_2$ fragments, or both.

Human memory B cells were negatively selected from peripheral blood and depleted of IgM + cells to yield CD19+ CD27+IgM^{neg} memory cells. We chose a negative selection procedure to isolate CD19+ IgM^{neg} peripheral blood memory B cells to avoid the potential activation of the B cells through binding of cell surface CD27 or crosslinking the BCR.(22) (23) These cells were then cultured for 96 hours with different stimulation conditions: medium alone (unstimulated), CpG+ cytokines (IL-2, IL-10, IL-15, BAFF) (CpG+CK), soluble anti-human IgG F(ab)$_2$ fragments of BCR-cross-linking antibody (BCR-x) or CpG+CK and BCR cross-linking (CpG+CK+BCR-x)) (n=6 wells, 300 live cells/well, 9 experiments). Parallel ELISPOT

and ELISA assays were seeded with washed cells and incubated for 4 hours, to capture spots from high σ_{IgG} cells most clearly, and 19 hours, to better assess spots with a low σ_{IgG}.

CpG+CK stimulated a large increase in the total number of IgG-SC as well as the fraction of cells secreting at a high σ_{IgG} (IgG>1000 fg•cell^{-1}) (Fig. 6a). Unstimulated IgG memory B cells and cells stimulated with soluble BCR-x alone produced very few spots, all within the low σ_{IgG} range (IgG<1000 fg•cell^{-1}), even at the longer 19 hour assay time. BCR cross-linking reduced the proportion of the IgG-secreting CpG+CK-stimulated IgM^{neg} B cells. In five experiments, the frequency of high σ_{IgG} IgG-SC was reduced by an average of 92.7 ± 4.73% and low σ_{IgG} IgG-SC by 53.3 ± 18.7%. This difference in reduction rates between the populations suggests that the low range σ_{IgG} IgG-SC spots detected are not merely background spots, but are spots produced by stimulated B cells. Multiple subpopulations within the major low and high σ_{IgG} IgG-SC subpopulation were also observed.

An increase in high-rate IgG-SC in memory B cell cultures stimulated with CpG+CK is associated with an increase in number of cell divisions and CD27 expression

Activation of memory B cells and initiation of IgG secretion has been shown to be division linked and associated with differentiation into B cell blast phenotype as measured by CD27 expression(24,25). Expecting a similar increase in the frequency of cells undergoing proliferation and differentiation, we stimulated CFSE-stained IgM^{neg} memory B cells with CpG+CK and/or soluble BCR-x for 72 hours and performed cytometric analyses.

B cells activated with CpG+CK showed more divisions than other stimuli tested after 72 hours; 2 divisions more than BCR-x and 1 division more than CpG+CK+ BCR-x (Fig. 6b). IgM^{neg} memory B cells cultured in medium alone did not have a clearly dividing population. An increase in cell surface expression of CD27, which is typical of B cell blast development, was seen with CpG+CK stimulation. The frequency of cells that had CD27 expression at higher levels than non-dividing CD27+ cells (CD27^{high}) increased with cell division (Undivided- 0.9 ± 0.03%, Div1 – 0.99± 0.45%, Div2 – 2.35 ± 1.19%, Div3 – 3.2 ± 2.1% (n=4 experiments). Reduced numbers of CD27^{high} cells were seen in CpG+ck+BCR-x cultures (Undivided – 0.91 ±0.096, Div1 – 0.18 ± 0.16%, Div2 – 0.22 ± 0.20%, Div3 – 0.39 ± 0.48%). Taken together with the decrease in high σ_{IgG} IgG-SC with the addition of BCR-x to CpG+CK stimulation, these data suggest that an increase in high σ_{IgG} IgG-SC with CpG+CK stimulation is due to an increase in frequency of the more differentiated CD27^{high} cells with each generation. This result appears to favor the secretion rate maturation hypothesis, in which activated memory B cells increase in range of σ_{IgG} with each division. This data also fit hypothesis 3 in which multiple subpopulations each respond to CpG+CK by increasing their secretion each within their own range. Reduced frequency of high σ_{IgG} IgG-SC and of CD27^{hi} B cells could be indicative of selective inhibition of one or more subpopulations of CpG+CK-stimulated memory B cell blasts by BCR cross-linking.

IL-21 stimulation induces development of a high σ_{IgG} IgG-SC population in CD40L-stimulated memory B cells

Interleukin-21 (IL-21) is a potent inducer of B cell proliferation and IgG production (26-28) and plays a critical role in activation of memory B cells by T cells(29), so we examined the effect of IL-21 stimulation on CD40L IgG-SG subpopulations. Human memory B cells, CD19 + CD27+ IgM^{neg}, were isolated as in figure 6a, CFSE-stained and co-cultured with CD40L-expressing NIH3T3 fibroblasts and IL-4. After 96 hours in culture, the cells were harvested, washed, and plated in parallel ELISPOT and ELISA assays for 19 hours. Spot size histograms and estimated IgG histograms are shown in figure 6c. IgM^{neg} memory B cells stimulated with CD40L and IL-4 produced low σ_{IgG} IgG-SC (<1000fg•cell^{-1}). Activation with CD40L + IL-21, or the addition of IL-21 to CD40L + IL-4 induced a small population of high σ_{IgG} IgG-SC not

seen in memory B cells stimulated with CD40L + IL-4 alone. Consistent with the widely-recognized mitogenic properties of IL-21, flow cytometric analyses of these cells showed that the addition of IL-21 to CD40L+IL-4 stimulation conditions increased the number of cell divisions from 3 to 5. An increase in the frequency of $CD27^{hi}$ cells was also observed with the addition of IL-21, particularly in divisions 4 and 5, suggesting that faster-dividing B cell blasts are associated with the appearance of functionally high σ_{IgG} IgG-SC. This strengthens the association between the presence of high σ_{IgG} IgG-SC and B cell blast phenotype subsets seen in figure 6a and b. Taken together, these data suggests that with more cell divisions, higher σ_{IgG} IgG-SC may develop, consistent with Hypotheses 1 or 3.

Increased cell death is seen in proliferating IgM^{neg} memory B cells with the addition of BCR-x to CPG+CK stimulation conditions

BCR cross-linking by soluble, bivalent $F(ab)_2$ fragments (BCR-x) has been shown to increase cell death in some B cell subsets and cell lines (20,30). To determine whether the reduced proportions of live proliferating B cell blasts, PB_{live}, in populations with the addition of BCR-x to CpG+CK stimulation was due to an increase in cell death, IgM^{neg} memory B cells were stained with CFSE, stimulated for 72 hours with CpG+CK, and stained for CD27 surface expression and live/dead violet dye (representative data Fig. 7; total n=6 experiments). A higher percentage of dead cells are seen in undivided populations in the CpG+CK stimulated cells (49.43 ± 0.21 %) than in CpG+CK+BCR-x stimulated cells (15.71± 0.08%; p=0.026). A large population of dead cells can be seen in Division 1 as well, but these may be undivided cells leaking CFSE into the Division 1 range. In contrast, more cell death is seen in division 3 with the addition of BCR-x to the CpG+CK stimulation (40.65 ± 0.02 %) as compared with CpG +CK alone (6.8 ± 0.03; p=0.000002) (n=4 experiments). This suggests that BCR-x selectively increased the rate of cell death in $CD27^{hi}$ memory B cell blasts and is in concordance with a reduction in total IgG production of the population through a decrease in frequency of PB_{live}.

Proliferating B cells in different generations secrete IgG with the same range of rates

To further test whether the secretion rate maturation hypothesis accurately reflected biology, we examined the σ_{IgG} of CFSE labeled IgM^{neg} memory B cells stimulated with CpG+CK for 72hrs. The cells were sorted by generation and CD27 surface expression, and analyzed for σ_{IgG} by qELISPOT. If, as the previous result suggests, IgG secretion rate increases with B cell blast generation number, we predicted we would find higher σ_{IgG} in $CD27^{high}$ cells in higher generations as compared with $CD27^{+}$ cells.

Figure 8a displays the IgG secretion profile of unsorted CpG+CK stimulated cells as well as the sorted populations (representative of n=3 experiments). Cells were sorted first into $CD27^{+}$ and $CD27^{high}$ populations. Then the cells were sorted again according to CFSE staining to isolate cells in each cell division. Live cells, at 300 per well and 6 wells per group, were assayed for IgG secretion (n=3 experiments). Fig. 8b shows that, contrary to the secretion rate maturation hypothesis, populations of $CD27^{high}$ B cell blasts in every generation had the same range of σ_{IgG} (division 1 vs. division 2 p=0.07; division 1 vs. division 3 p=0.06; division 2 vs. division 3 p=0.14). Only the frequency of IgG-SC increased with cell division.

Not all cells, even in divisions 3 and 4, however, secreted IgG after CpG+CK activation. There was a persistent population of $CD27^{+}$ memory B cells that did not secrete IgG present in each division. Even in Divisions 3 and 4, only 47.2% of live $CD27^{high}$ cells were detectable IgG-SC. IgA-positive cells were found comprise 4-11% of CD27+ IgM^{neg} memory cells activated with CpG+CK for 72 hours, which does not account for cells not producing IgG. (data not shown). This suggests that after 72 hours of CpG+CK stimulation, more than half of memory B cells that are proliferating and increasing CD27 surface expression are not secreting IgG or are secreting at levels much lower than the sensitivity of the qELISPOT assay.

Secretion of IgG is a multi-step process that involves production of intracellular IgG before release from the cell. To determine if a delay or block in release of IgG from a proportion of CpG+CK activated CD27+ IgM^{neg} memory cells lead to non-secreting populations not detectable by the qELISPOT assay, flow cytometric analysis was performed using CFSE, BrdU incorporation and intracellular IgG staining. Representative data in Fig. 8 show that the frequency of cells positive for intracellular IgG increased with division class (n=3 separate experiments). This paralleled the increase in IgG secreting cells measured by qELISPOT. This data suggests that the lack of IgG secretion in cells not detected by qELISPOT is likely due to a lack of IgG production.

Considered with the result that IgG secretion range is independent of generation in memory B cell blasts, selective cell death of memory B cell blasts when treated with BCR-crosslinker indicates that at least two processes can occur: a change in the relative populations of high- and low-rate IgG producing cells, and an increase of the frequency of IgG-SC within a population. This data, in aggregate, favors hypothesis 3 in which total IgG secretion is the combined product of the contributions of multiple populations of IgG-SC.

Discussion

In a memory B cell recall response, the total amount of antibody secreted by the activated memory B cells over time can be modulated by changes in the percentage of antibody secreting cells (φ_{ASC}), changes in the rate at which they secrete antibody (σ_{IgG}), or changes in the proportion of live cells (PB_{live}) (Figure 1a). Previous experimental methods have not had the ability to resolve these terms at the single cell level to determine the population distribution of these rates. Particularly problematic has been measurement of σ_{IgG}, the rate of IgG secretion per individual cell. IgG secretion rates have routinely been measured by assaying total IgG accumulated in culture supernatants over 7-14 days, deriving single cell secretion rates by dividing the total IgG measured by the number of cells found to be secreting IgG by ELISPOT, or even less accurately, but the total number of cells in the culutre (31). As B cells may divide but not secrete IgG, or may undergo apoptosis, this approach cannot capture the single cell dynamics of IgG secretion in multiple subpopulations of B cells that proliferate, secrete IgG, and die over that time. Distinguishing between such behaviors is, however, crucial to understanding how a population of activated memory B cells functions to survive, produce IgG, and clonally expand memory B cells during secondary B cell immune responses. This analysis is particularly important if the B cell populations comprise functionally distinct populations with different antibody secretion rates. It has direct implications for vaccine design if different adjuvants, live attenuated, or recombinant vaccine formulations produce different proportions of ASC with different immunoglobulin secretion rates.

To determine the differential effects of φ_{ASC} and σ_{IgG} on IgG production early in memory B cell activation, we measured the σ_{IgG} of single activated memory B cells within a large population. In this system, CpG ODN activation resulted in 70-80% of IgG+ CD27+ memory B cells cycling through successive rounds of mitosis, but only 17-47% secreting immunoglobulin. Our finding that less than 50% of memory B cells in these assays secrete IgG is in agreement with earlier studies (25). Of those cells secreting immunoglobulin, we estimated that individual cell IgG secretion rates varied between 10-10^5 fg/cell, also a function of cell culture conditions.

Quantitative ELISPOT showed a marked heterogeneity of σ_{IgG} in CpG+CK stimulated cells, coupled with a striking bimodal distribution of σ_{IgG}. Two functionally distinct populations of IgG-SC were apparent, a low σ_{IgG} group at approximately 10-10^3 fg IgG•$cell^{-1}$ •4 $hours^{-1}$ and a high σ_{IgG} group with secretion rates 10^3-10^5 fg IgG•$cell^{-1}$ •4 $hours^{-1}$. These measurements are in the same range as previous estimates of average IgG secretion rates estimated by

immunoaffinity capillary electrophoresis with laser-induced fluorescence detection (32) and ^{35}S protein labeling (33). The qELISPOT method could easily be used to measure secretion rates of other proteins as well, such as other immunoglobulin subtypes or cytokines.

We report here that two distinct signaling pathways, TLR-9 signaling with CpG DNA in the context of IL-2, IL-6, IL-10 and BAFF versus CD40L signaling in the context of IL-4, give rise to different rates of IgG secretion and different frequencies of antibody secreting B cell blasts. We also found that high σ_{IgG} cells are induced in memory B cells when exogenous IL-21 was added to CD40L+IL-4 stimulation. In agreement with previous studies in which switched memory B cells responded to CD40L and IL-21 with increased proliferation(26,29,34), increased IL-6 and IL-10 secretion(26), and increased Ig secretion (29,34), we found that IL-21 gave rise to an increase in proliferation and development of a functionally distinct population of high σ_{IgG} cells. Further experiments are planned to examine differences in BAFF signaling and other plasma-cell associated genes in high σ_{IgG} B cells.

An interesting finding was that soluble $F(ab)_2$ cross-linking of the B cell receptor during CpG +CK B cell activation resulted in fewer cycles of cell division, modulated IgG secretion by reducing IgG secreting B cell blasts (φ_{ASC}) and increased cell death in proliferating B cell blasts. As we used $F(ab)_2$ fragments for BCR cross-linking, this effect was independent of FcγIIRb signaling, which also down-regulates IgG secretion. (35) Work in mice has shown that BCR stimulation can interfere with CpG activation of B cells by TLR agonists such as CpG (21) and LPS (36,37) and interfere with CpG-mediated plasma cell development (21). This may be through BCR-mediated ERK signaling. (21,38) Also, NF-κB activation is prolonged in mouse WEHI cells when CpG and anti-IgM stimuli are combined. (39) We found that functionally different subpopulations of IgG-secreting memory B cells, as visualized with the quantitative ELISPOT assay, result from BCR-stimulated interference in CpG-stimulated plasmablast development. Future investigation will be needed to define the precise conditions for this effect and address the cell signalling pathways that are involved.

An important finding is that after three days of CpG+CK stimulation, memory B cells that have divided at least once will secrete IgG with a similar distribution of IgG secretion rates, independent of their division class. Thus, IgG secretion appears to be a binary switch, rather than a type of secretion maturation in which cells secrete IgG at lower rates in earlier generations and higher rates at later generations. We found that the range and distribution of σ_{IgG} under various stimulation conditions is the same, but the φ_{ASC} increases with cell division. These findings, taken together, support the “mixture” hypothesis of total antibody secretion, in which the frequency of dividing cells and the “on/off” IgG secretion switch determine the φ_{ASC} for multiple populations of ASC that secrete IgG at different per-cell rates (σ_{IgG}). While the current data suggest two major subpopulations for σ_{IgG}, different *in vivo* and experimental conditions may yield more subpopulations with different distributions of σ_{IgG}. Further work will be needed to demonstrate that B cell responses to the in vitro stimulation conditions used here, CpG+CK and CD40L+IL-4, are comparable to those seen in vivo, although we have found similar antibody secretion rates in human peripheral blood B cells 7 days after influenza immunization.

An “on/off” modulation of IgG secretion is consistent with a stochastic switching mechanism. These experiments do not, however, allow us to determine if cell division is asymmetric, with one daughter cell differentiating into an antibody secreting cell, and the second into a dividing memory B cell, as some have proposed (40). However, we did find that non-IgG secreting B cells still proliferated at the same rate as their IgG-producing counterparts, suggesting that under the conditions tested IgG secretion does not impede cell division. It was also not possible however, given the limitations of the experimental method, to determine if differentiation into an IgG secreting phenotype is a unidirectional event, or if IgG secreting cells can de-

differentiate into a non-secreting phenotype in subsequent divisions. Whether these non-IgG secreting B cell blasts eventually replenish the stable resting memory B cell pool will require further work *in vivo*.

Sorting CpG+CK-stimulated memory B cells by division and CD27 expression, we found a lower φ_{ASC} in CD27+ memory cells as compared with $CD27^{high}$ cells. However, the division between CD27+ and $CD27^{high}$ cells was set using the CD27 expression level of non-dividing cells, so $CD27^{high}$ B cell blasts may have been sorted in these studies as CD27+. In this case, all of the IgG spots could be attributed to B cell blasts. This heterogeneity of IgG secretion is similar to the heterogeneity of CD27 and CD38 expression previously reported. (25) Blimp-1 expression, a hallmark of antibody secreting cells, is seen in B cells with heterogeneous Ig secretion rates (41). With the qELISPOT method, it will be possible to examine correlations between IgG secretion and other factors that affect IgG secretion at the single cell and population-wide levels. It will also be possible to model more accurately the complex interactions between cell division, cell death, φ_{ASC}, and σ_{IgG} in B cell population dynamics. These questions are beyond the scope of this manuscript, and are the subjects of future investigations.

In summary, comparing the results from CD27 and division class sorted B cells with the differences seen between memory B cell populations stimulated with different culture conditions, we conclude that there are at least two processes that can modulate IgG secretion: a change in the relative populations of high- and low- IgG antibody secretion rate σ_{IgG} cells, and an increase of the frequency of IgG-SC (φ_{ASC}) within a population that is independent of division number. The combined data support the hypothesis that the total amount of IgG secretion in a population of CpG+CK activated memory B cells is regulated by the relative contributions of multiple subpopulations of IgG secreting (“switched on”) B cell blasts, each with a distinct IgG secretion rate distribution.

Acknowledgements

We would like to thank Xia Jin, Hulin Wu, David Topham, Ignacio Sanz,, and the members of the University of Rochester Center for Biodefense Immune Modeling for spirited discussions which greatly improved the manuscript.

Abbreviations used in this paper

PB_{live}, total number of living cells
φ_{ASC}, fraction of cells secreting IgG
σ_{IgG}, rate at which IgG is secreted by each cell
ASC, Ab-secreting cell
BAFF, B cell activating factor
BCR-x, BCR cross-linking Ab
CpG plus CK, CpG and cytokines
ODN, oligodeoxynucleotide
DSB, desthiobiotin
IgG-SC, IgG-secreting cell
Int-U, intensity unit
qELISPOT, quantitative ELISPOT
rhuIL, human rIL
t_{inc}, incubation time

References

1. Tangye SG, Avery DT, Hodgkin PD. A division-linked mechanism for the rapid generation of Ig-secreting cells from human memory B cells. J Immunol 2003;170:261–269. [PubMed: 12496408]

2. Hemmi H, Takeuchi O, Kawai T, Kaisho T, Sato S, Sanjo H, Matsumoto M, Hoshino K, Wagner H, Takeda K, Akira S. A Toll-like receptor recognizes bacterial DNA. Nature 2000;408:740–745. [PubMed: 11130078]
3. Bernasconi NL, Traggiai E, Lanzavecchia A. Maintenance of serological memory by polyclonal activation of human memory B cells. Science 2002;298:2199–2202. [PubMed: 12481138]
4. Huggins J, Pellegrin T, Felgar RE, Wei C, Brown M, Zheng B, Milner EC, Bernstein SH, Sanz I, Zand MS. CpG DNA activation and plasma-cell differentiation of CD27- naive human B cells. Blood 2007;109:1611–1619. [PubMed: 17032927]
5. Shiao RT, McLeskey SB, Khera SY, Wolfson A, Freter CE. Mechanisms of inhibition of IL-6-mediated immunoglobulin secretion by dexamethasone and suramin in human lymphoid and myeloma cell lines. Leukemia & lymphoma 1996;21:293–303. [PubMed: 8726410]
6. Manzer DS, Littlefield BA. Stimulation of IgG production by glucocorticoids in human myeloma lymphoblasts. Biochimica et biophysica acta 1988;969:40–47. [PubMed: 3349108]
7. al-Rubeai M, Emery AN. Mechanisms and kinetics of monoclonal antibody synthesis and secretion in synchronous and asynchronous hybridoma cell cultures. Journal of biotechnology 1990;16:67–85. [PubMed: 1366816]
8. Leibson PJ, Loken MR, Panem S, Schreiber H. Clonal evolution of myeloma cells leads to quantitative changes in immunoglobulin secretion and surface antigen expression. Proc Natl Acad Sci U S A 1979;76:2937–2941. [PubMed: 288078]
9. Ma CS, Hodgkin PD, Tangye SG. Automatic generation of lymphocyte heterogeneity: Division-dependent changes in the expression of CD27, CCR7 and CD45 by activated human naive CD4+ T cells are independently regulated. Immunology and cell biology 2004;82:67–74. [PubMed: 14984597]
10. Hasbold J, Corcoran LM, Tarlinton DM, Tangye SG, Hodgkin PD. Evidence from the generation of immunoglobulin G-secreting cells that stochastic mechanisms regulate lymphocyte differentiation. Nature immunology 2004;5:55–63. [PubMed: 14647274]
11. Czerkinsky CC, Nilsson LA, Nygren H, Ouchterlony O, Tarkowski A. A solid-phase enzyme-linked immunospot (ELISPOT) assay for enumeration of specific antibody-secreting cells. J Immunol Methods 1983;65:109–121. [PubMed: 6361139]
12. Rebhahn JA, Bishop C, Divekar AA, Jiminez-Garcia K, Kobie JJ, Lee FE, Maupin GM, Snyder-Cappione JE, Zaiss DM, Mosmann TR. Automated analysis of two- and three-color fluorescent Elispot (Fluorospot) assays for cytokine secretion. Comput Methods Programs Biomed 2008;92:54–65. [PubMed: 18644656]
13. Zand MS, Vo T, Pellegrin T, Felgar R, Liesveld JL, Ifthikharuddin JJ, Abboud CN, Sanz I, Huggins J. Apoptosis and complement-mediated lysis of myeloma cells by polyclonal rabbit antithymocyte globulin. Blood 2006;107:2895–2903. [PubMed: 16368890]
14. Zand MS, Bose A, Vo T, Coppage M, Pellegrin T, Arend L, Lee FE, Bozorgzadeh A, Leong N. A renewable source of donor cells for repetitive monitoring of T- and B-cell alloreactivity. Am J Transplant 2005;5:76–86. [PubMed: 15636614]
15. Shah A, Nadasdy T, Arend L, Brennan J, Leong N, Coppage M, Orloff M, Demme R, Zand MS. Treatment of C4d-positive acute humoral rejection with plasmapheresis and rabbit polyclonal antithymocyte globulin. Transplantation 2004;77:1399–1405. [PubMed: 15167598]
16. Hollander, M.; Wolf, DA. Nonparametric Statistical Methods. Wiley; New York: 1999.
17. Krieg AM, Yi AK, Matson S, Waldschmidt TJ, Bishop GA, Teasdale R, Koretzky GA, Klinman DM. CpG motifs in bacterial DNA trigger direct B-cell activation. Nature 1995;374:546–549. [PubMed: 7700380]
18. Goeckeritz BE, Flora M, Witherspoon K, Vos Q, Lees A, Dennis GJ, Pisetsky DS, Klinman DM, Snapper CM, Mond JJ. Multivalent cross-linking of membrane Ig sensitizes murine B cells to a broader spectrum of CpG-containing oligodeoxynucleotide motifs, including their methylated counterparts, for stimulation of proliferation and Ig secretion. Int Immunol 1999;11:1693–1700. [PubMed: 10508187]
19. Bernasconi NL, Onai N, Lanzavecchia A. A role for Toll-like receptors in acquired immunity: up-regulation of TLR9 by BCR triggering in naive B cells and constitutive expression in memory B cells. Blood 2003;101:4500–4504. [PubMed: 12560217]

20. Yi AK, Yoon JG, Krieg AM. Convergence of CpG DNA- and BCR-mediated signals at the c-Jun N-terminal kinase and NF-kappaB activation pathways: regulation by mitogen-activated protein kinases. Int Immunol 2003;15:577–591. [PubMed: 12697659]
21. Rui L, Vinuesa CG, Blasioli J, Goodnow CC. Resistance to CpG DNA-induced autoimmunity through tolerogenic B cell antigen receptor ERK signaling. Nat Immunol 2003;4:594–600. [PubMed: 12740574]
22. Nagumo H, Agematsu K, Shinozaki K, Hokibara S, Ito S, Takamoto M, Nikaido T, Yasui K, Uehara Y, Yachie A, Komiyama A. CD27/CD70 interaction augments IgE secretion by promoting the differentiation of memory B cells into plasma cells. J Immunol 1998;161:6496–6502. [PubMed: 9862673]
23. Arens R, Nolte MA, Tesselaar K, Heemskerk B, Reedquist KA, van Lier RA, van Oers MH. Signaling through CD70 regulates B cell activation and IgG production. J Immunol 2004;173:3901–3908. [PubMed: 15356138]
24. Tangye SG, Ferguson A, Avery DT, Ma CS, Hodgkin PD. Isotype switching by human B cells is division-associated and regulated by cytokines. J Immunol 2002;169:4298–4306. [PubMed: 12370361]
25. Avery DT, Ellyard JI, Mackay F, Corcoran LM, Hodgkin PD, Tangye SG. Increased expression of CD27 on activated human memory B cells correlates with their commitment to the plasma cell lineage. J Immunol 2005;174:4034–4042. [PubMed: 15778361]
26. Good KL, Bryant VL, Tangye SG. Kinetics of human B cell behavior and amplification of proliferative responses following stimulation with IL-21. J Immunol 2006;177:5236–5247. [PubMed: 17015709]
27. Jin H, Carrio R, Yu A, Malek TR. Distinct activation signals determine whether IL-21 induces B cell costimulation, growth arrest, or Bim-dependent apoptosis. J Immunol 2004;173:657–665. [PubMed: 15210829]
28. Ozaki K, Spolski R, Feng CG, Qi CF, Cheng J, Sher A, Morse HC 3rd, Liu C, Schwartzberg PL, Leonard WJ. A critical role for IL-21 in regulating immunoglobulin production. Science 2002;298:1630–1634. [PubMed: 12446913]
29. Kuchen S, Robbins R, Sims GP, Sheng C, Phillips TM, Lipsky PE, Ettinger R. Essential role of IL-21 in B cell activation, expansion, and plasma cell generation during CD4+ T cell-B cell collaboration. J Immunol 2007;179:5886–5896. [PubMed: 17947662]
30. Yan BC, Adachi T, Tsubata T. ER stress is involved in B cell antigen receptor ligation-induced apoptosis. Biochem Biophys Res Commun 2008;365:143–148. [PubMed: 17976372]
31. Engvall E, Perlmann P. Enzyme-linked immunosorbent assay, Elisa. 3. Quantitation of specific antibodies by enzyme-labeled anti-immunoglobulin in antigen-coated tubes. J Immunol 1972;109:129–135. [PubMed: 4113792]
32. Phillips TM. Analysis of single-cell cultures by immunoaffinity capillary electrophoresis with laser-induced fluorescence detection. Luminescence 2001;16:145–152. [PubMed: 11312540]
33. de Grandmont MJ, Racine C, Roy A, Lemieux R, Neron S. Intravenous immunoglobulins induce the in vitro differentiation of human B lymphocytes and the secretion of IgG. Blood 2003;101:3065–3073. [PubMed: 12480708]
34. Bryant VL, Ma CS, Avery DT, Li Y, Good KL, Corcoran LM, de Waal Malefyt R, Tangye SG. Cytokine-mediated regulation of human B cell differentiation into Ig-secreting cells: predominant role of IL-21 produced by CXCR5+ T follicular helper cells. J Immunol 2007;179:8180–8190. [PubMed: 18056361]
35. Jiang Y, Hirose S, Sanokawa-Akakura R, Abe M, Mi X, Li N, Miura Y, Shirai J, Zhang D, Hamano Y, Shirai T. Genetically determined aberrant down-regulation of FcgammaRIIB1 in germinal center B cells associated with hyper-IgG and IgG autoantibodies in murine systemic lupus erythematosus. Int Immunol 1999;11:1685–1691. [PubMed: 10508186]
36. Kearney JF, Cooper MD, Lawton AR. B lymphocyte differentiation induced by lipopolysaccharide. III. Suppression of B cell maturation by anti-mouse immunoglobulin antibodies. J Immunol 1976;116:1664–1668. [PubMed: 1083879]
37. Schliephake DE, Schimpl A. Blimp-1 overcomes the block in IgM secretion in lipopolysaccharide/anti-mu F(ab')2-co-stimulated B lymphocytes. Eur J Immunol 1996;26:268–271. [PubMed: 8566078]

38. Rui L, Healy JI, Blasioli J, Goodnow CC. ERK signaling is a molecular switch integrating opposing inputs from B cell receptor and T cell cytokines to control TLR4-driven plasma cell differentiation. J Immunol 2006;177:5337–5346. [PubMed: 17015719]

39. Yi AK, Krieg AM. CpG DNA rescue from anti-IgM-induced WEHI-231 B lymphoma apoptosis via modulation of I kappa B alpha and I kappa B beta and sustained activation of nuclear factor-kappa B/c-Rel. J Immunol 1998;160:1240–1245. [PubMed: 9570540]

40. Tangye SG, Hodgkin PD. Divide and conquer: the importance of cell division in regulating B-cell responses. Immunology 2004;112:509–520. [PubMed: 15270721]

41. Kallies A, Hasbold J, Tarlinton DM, Dietrich W, Corcoran LM, Hodgkin PD, Nutt SL. Plasma cell ontogeny defined by quantitative changes in blimp-1 expression. J Exp Med 2004;200:967–977. [PubMed: 15492122]

a.

$$IgG = \int_{t=0}^{t_{inc}} PB_{live} \cdot \phi_{ASC} \cdot \sigma_{IgG} \cdot dt$$

b.

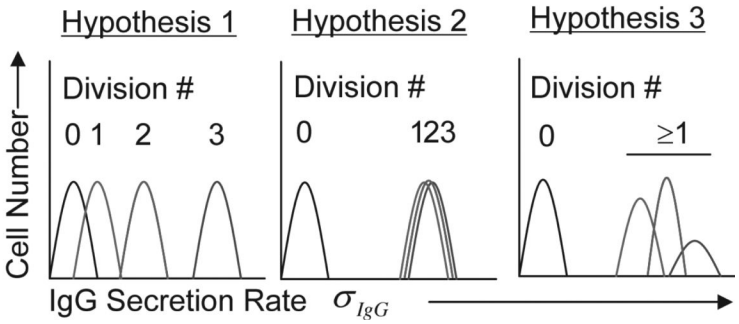

Figure 1a. An equation to describe how individual B cells contribute to total IgG production within a population

IgG is the total IgG secreted, PB_{live} is the number of live B cell blasts, φ_{ASC} is the fraction of live cells that are secreting IgG, σ_{IgG} is the rate of IgG secretion per cell, t is time and t_{inc} is the incubation time of the assay. 1b. Hypotheses for the relationship between cell division and IgG secretion range of B cell populations. The secretion rate maturation hypothesis posits that memory B cells stimulated to differentiate into B cell blasts increase their σ_{IgG} with each subsequent mitosis such that cells that have divided more times secrete IgG at a higher σ_{IgG}. An alternative possibility is that σ_{IgG} are independent of division class, behaving more like a binary "On/Off" switch. In this model, dividing cells secrete IgG in the same range, irregardless of division number and control of population IgG secretion is asserted through control of φ_{ASC}. In the third "mixture" hypothesis, several subpopulations of memory B cell blasts produce different σ_{IgG} distributions.

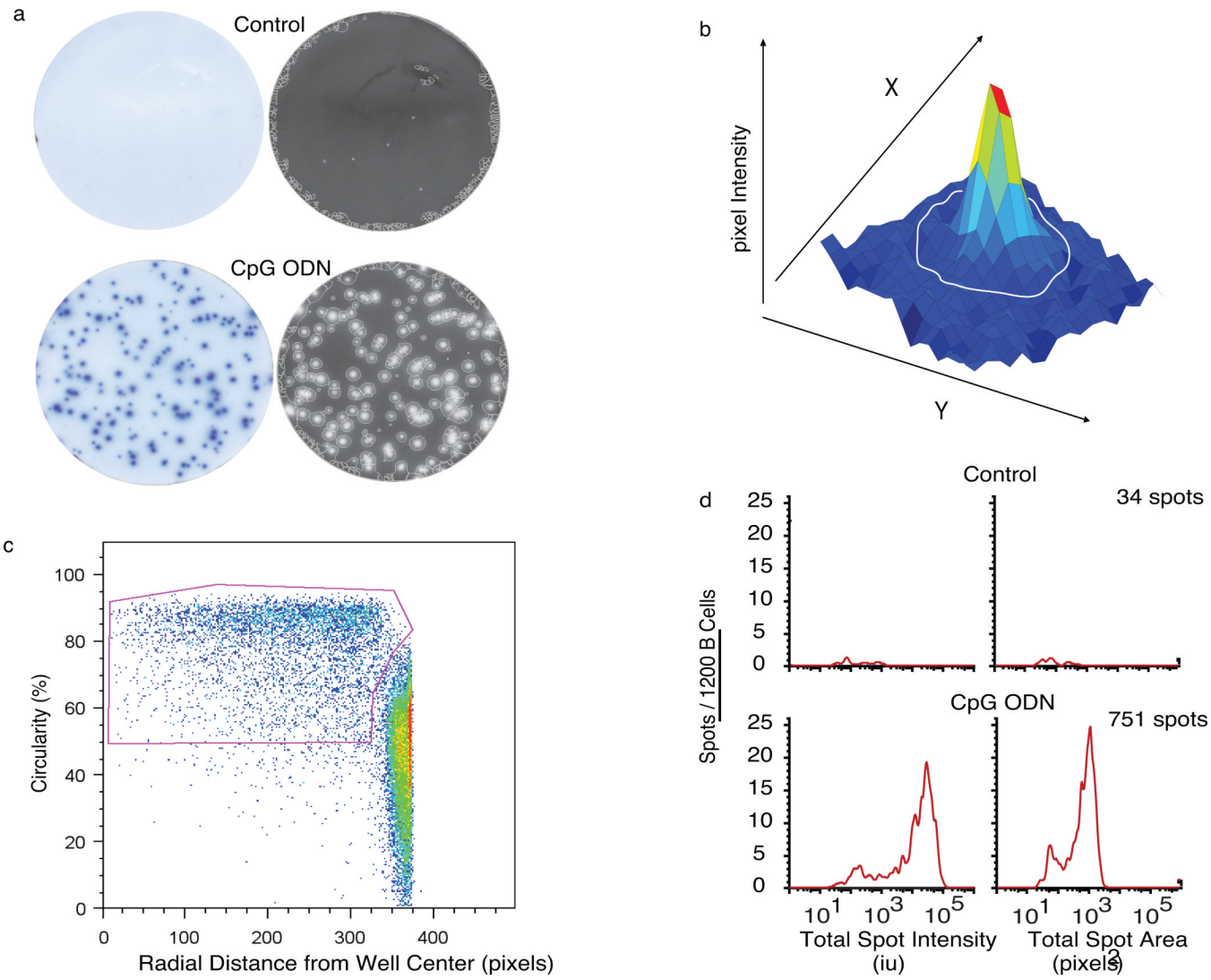

Figure 2. Bimodal Distribution of the IgG ELISPOTs in CpG+CK-stimulated memory B cells

Unstimulated and CpG+CK-stimulated human IgG depleted CD27+ memory B cells, were incubated in ELISPOT plates for 6 hours. (a) Raw and EXPLORAspot-processed representative ELISPOT well images selected from 9 independent experiments (3-6 replicate wells per experiment) show that CpG+CK-stimulation increased the amount of IgG secreted as well as the number of cells secreting IgG ($p<0.001$). The EXPLORAspot software detected the circled spots. To eliminate well-edge artifacts, all spots data from each 96 well plate were pooled and FACS analysis software used to create a bivariate plot of the radial distance of each spot from the center of the well versus spot circularity. (b) A three-dimensional plot showing x and y coordinates used for spot area calculation. Spot intensity is the sum of spot pixel values (defined in arbitrary intensity units: Int-U) which are represented here by the z-axis. (c) Gating strategy that maximized retention of circular "true" spots at well edges, while eliminating less circular well edge artifact. (d) Histograms of pooled spot populations from 6 replicate wells including the wells pictured in 2a showing that spot numbers increased 20-fold in response to CpG+CK stimulation. Spot total intensity values also increase with some heterogeneity in IgG spot sizes over the population.

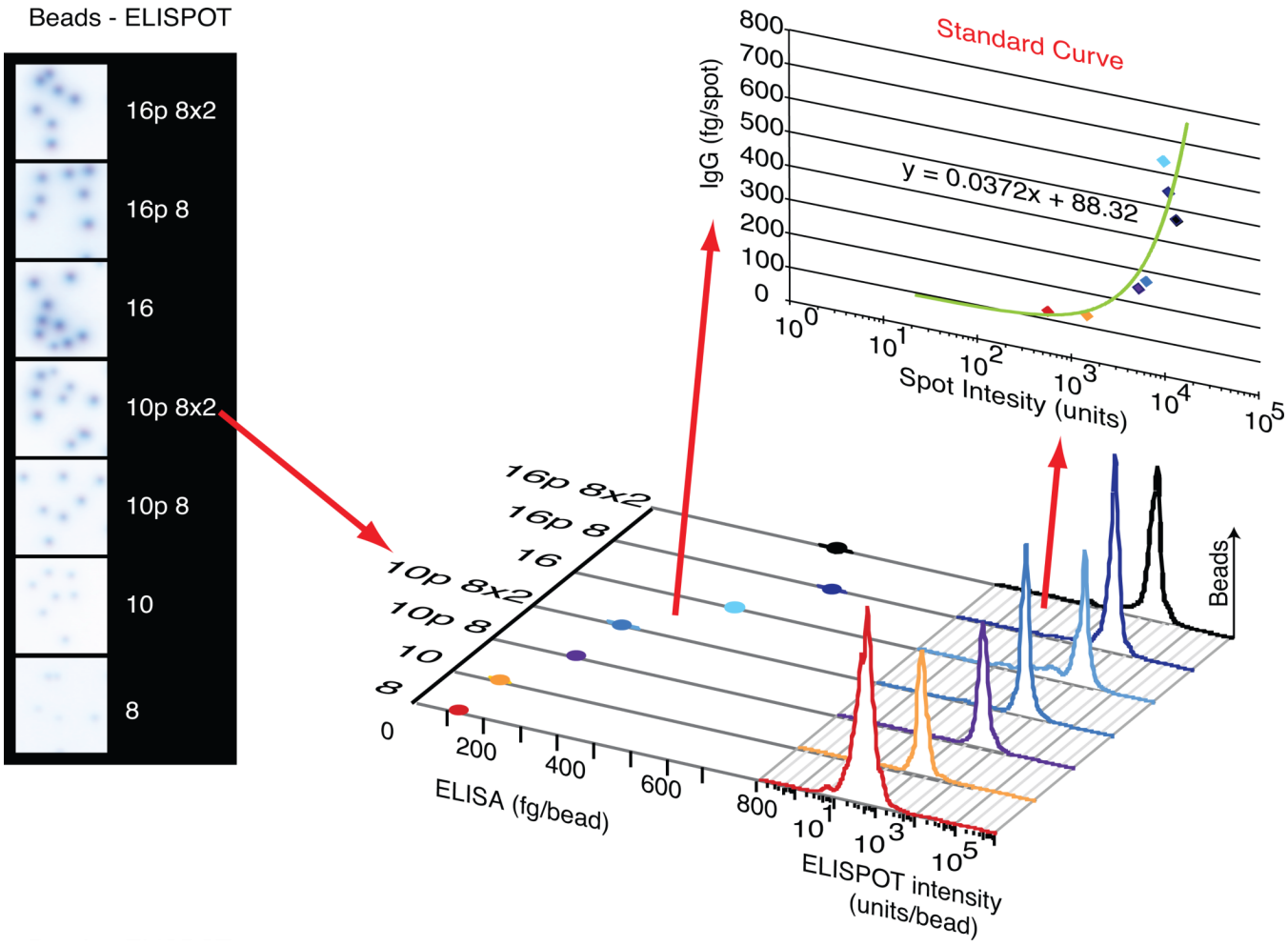

Figure 3. Bead-mediated Estimation of IgG Release

Sampled well images with spots produced by human IgG released from different sizes of polymer beads. Spot size and ELISA data quantitating IgG release from the same bead samples were plotted to construct a standard curve describing the mathematical relationship between spot size and IgG released per bead. This standard curve could then be used to assign absolute IgG secretion rates to individual spots in the experiment.

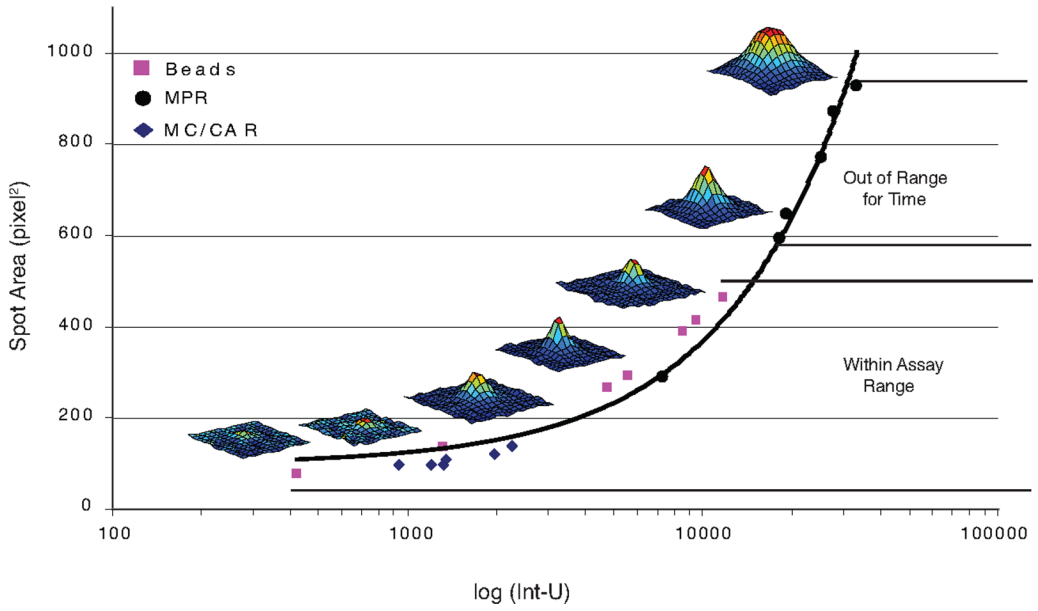

Figure 4. The mathematical relationship between the spot area and total intensity

The means of the areas and total spot intensity values of spots generated by low-rate (MC/CAR) and high-rate (MPR1130) IgG-secreting control myeloma cells lines as well as IgG-releasing beads were compared. A direct relationship between spot area and total intensity can be seen, whether the spot was formed by cells or by beads. Therefore, either parameter could be used for comparison to IgG released by ELISA. Three-dimensional well images indicating changes in spot morphology with increasing spot size are also shown.

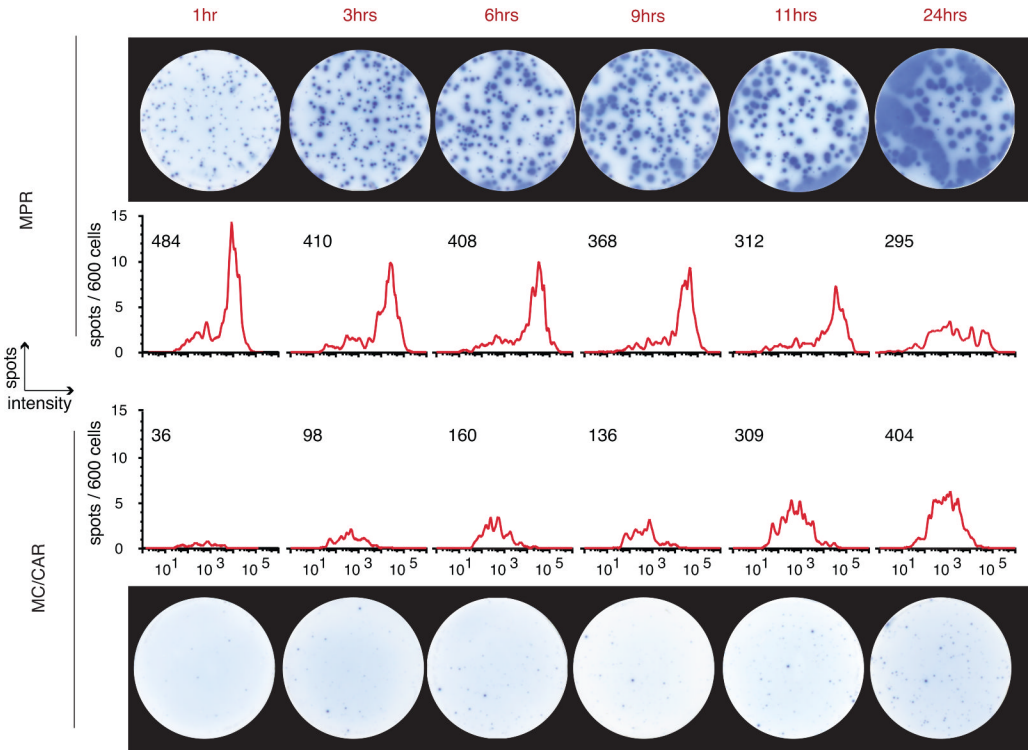

Figure 5. Spot Development Over Time of Incubation (t_{inc})

A time course showing well images and matching spot intensity histograms of two myeloma cell lines secreting IgG at a high and a low rate. At time points beyond 6 hours, spots detected from the high-rate secreting cell line MPR spot begin to merge and then cannot be accurately analyzed. Beyond 12 hours, the low-secreting myeloma cells are still producing spots that are coming into detectable range of sizes, so time is a critical factor in these studies. The effective range of total spot intensity values detected was 30 to 2×10^5 INT-U.

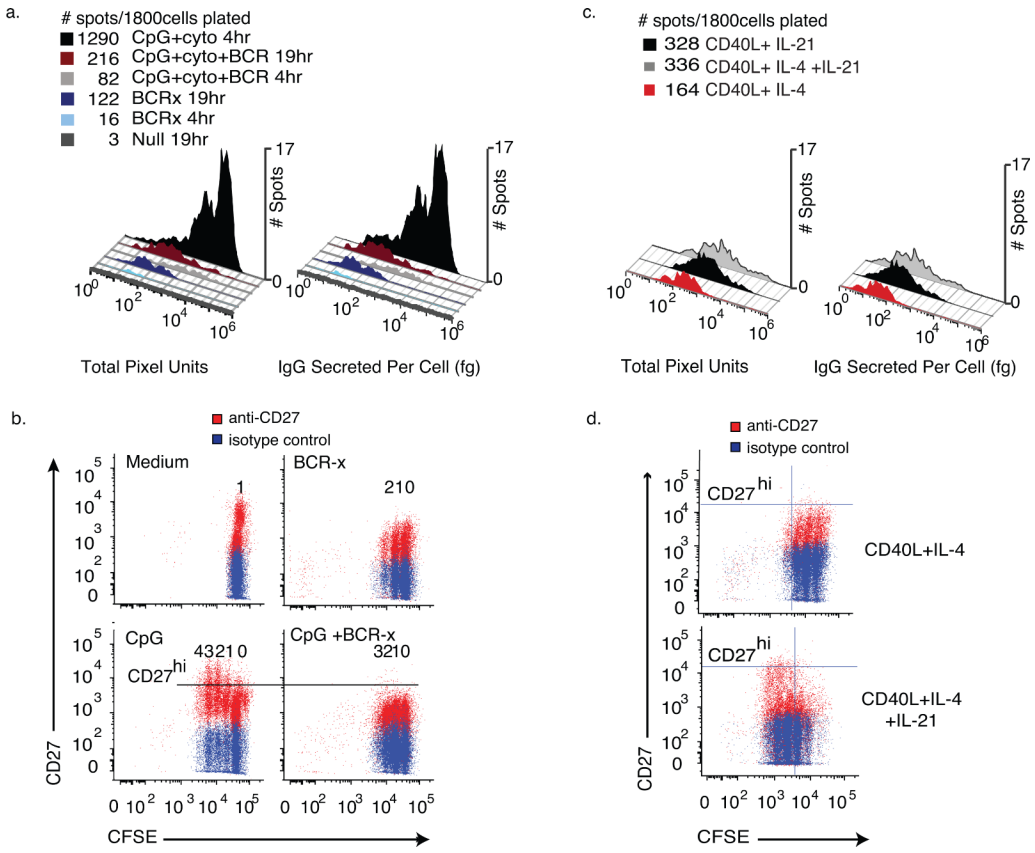

Figure 6. Estimating IgG release from individual cells in mixed populations of responding memory B cells

Human CD27+ memory cells depleted of IgM+ B cells were isolated and split into groups cultured with medium, CpG_{2006} ODN and cytokines (CpG+ck) and BCR-crosslinking antibodies (BCR-x), alone or in combination. After 96 hours of culture, the cells were washed and assayed for IgG secretion in paired ELISA and ELISPOT assays next to wells pre-spotted with bead standards for IgG release. Cells were incubated in the assay plates for 4 hours or 19hours (N=6wells, 300 live cells/well). Using a bead-derived standard curve as in Fig. 4, values for IgG secreted were calculated. (a) Histograms of raw spot intensity and estimated IgG secretion. The addition of BCR-crosslinking antibodies to the CpG+CK stimulation conditions reduced the number of high- σ_{IgG} IgG-SC by 92.7 ± 4.73% and low range σ_{IgG} IgG-SC by 53.3 ± 18.7%. Spots on plates allowed to incubate 19hrs show low σ_{IgG} (IgG<1000 fg•cell^{-1}) cell populations more clearly. (b) Flow cytometric analysis of IgM^{neg} memory B cells stained with CFSE at isolation, stimulated with CpG+CK stained for viability and CD27 cell surface marker expression after 72 hours of incubation. Undivided cells are seen as the population furthest to the right, each division producing an additional population with reduced CFSE staining. With each generation, an increase in $CD27^{high}$ proliferating B cell blasts can be seen in CpG+CK-stimulated cells and the number of $CD27^{high}$ cells is reduced by the addition of BCR-x. (c) Spot Intensity and estimated IgG secreted per cell histograms of IgM-depleted CD19+CD27+ memory B cells that had been stimulated with CD40L-expressing fibroblasts and rhuIL-4 or rhuIL-21, alone or in combination for 96 hours, washed and assayed as in figure 6a. CD40L and IL-4 stimulation yielded low σ_{IgG} IgG-SC. Activation by CD40L +IL-21, with or without IL-4 induced a small population of high σ_{IgG} IgG-SC and increased total spot numbers. (d) CFSE vs CD27 expression of cells treated as in (c). In cell populations

treated with IL-21, more cell division is evident and CD27 expression increases in dividing cells, consistent with development of a B cell blast phenotype.

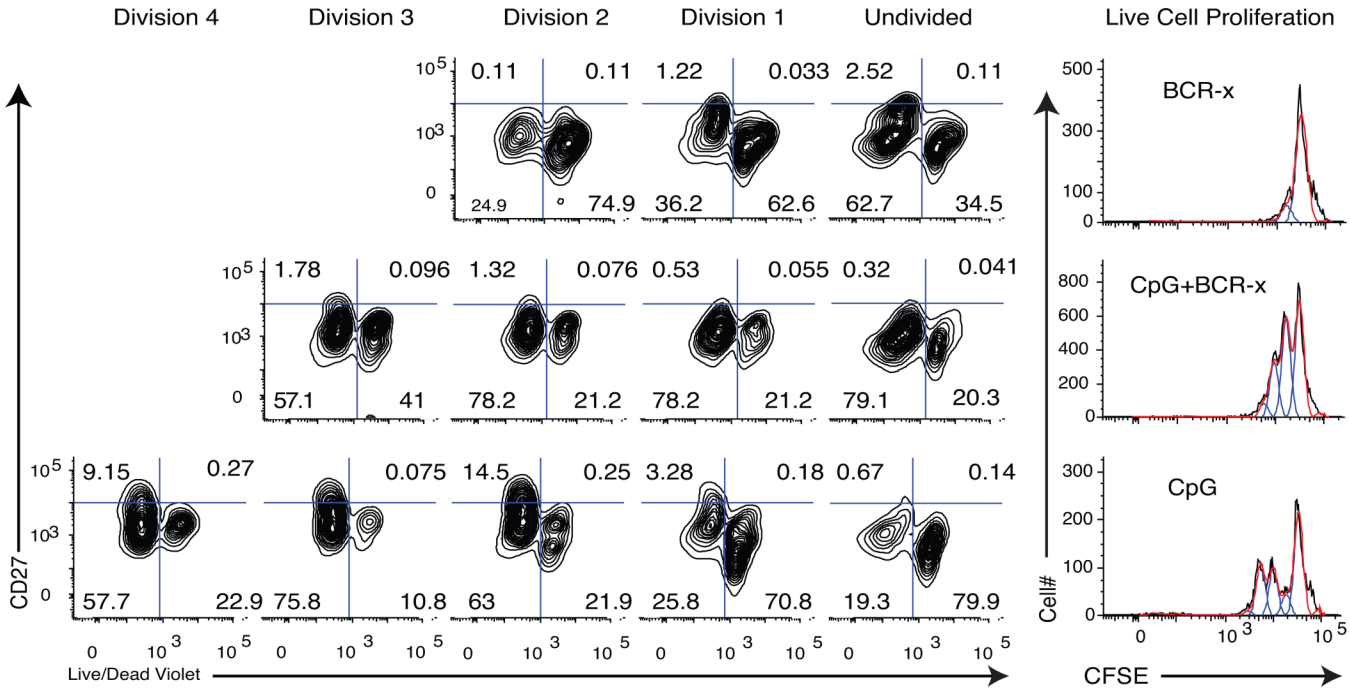

Figure 7. Increased cell death in later divisions of CpG+CK+BCR-x stimulated cells

IgM^{neg} memory B cells were isolated from the donor and split into treatment groups, with medium alone (Unstimulated), BCR-x, CpG+CK, and CpG+CK+BCR-x. After 72 hours in culture, the cells were stained for cell surface CD27 and live/dead violet dye (representative of 3 experiments). Dead cells retain this dye, appearing to the right in these figures. CpG+CK treatment produced more dead cells in Undivided and Division 1 populations. Addition of BCR-x to CpG+CK changed this profile to favor more live cells in undivided populations and more dead cells in later divisions. This suggests that reduced numbers of high-rate IgG-SC and reduced B cell blasts in CpG+CK+BCR-x may be due to higher death rates.

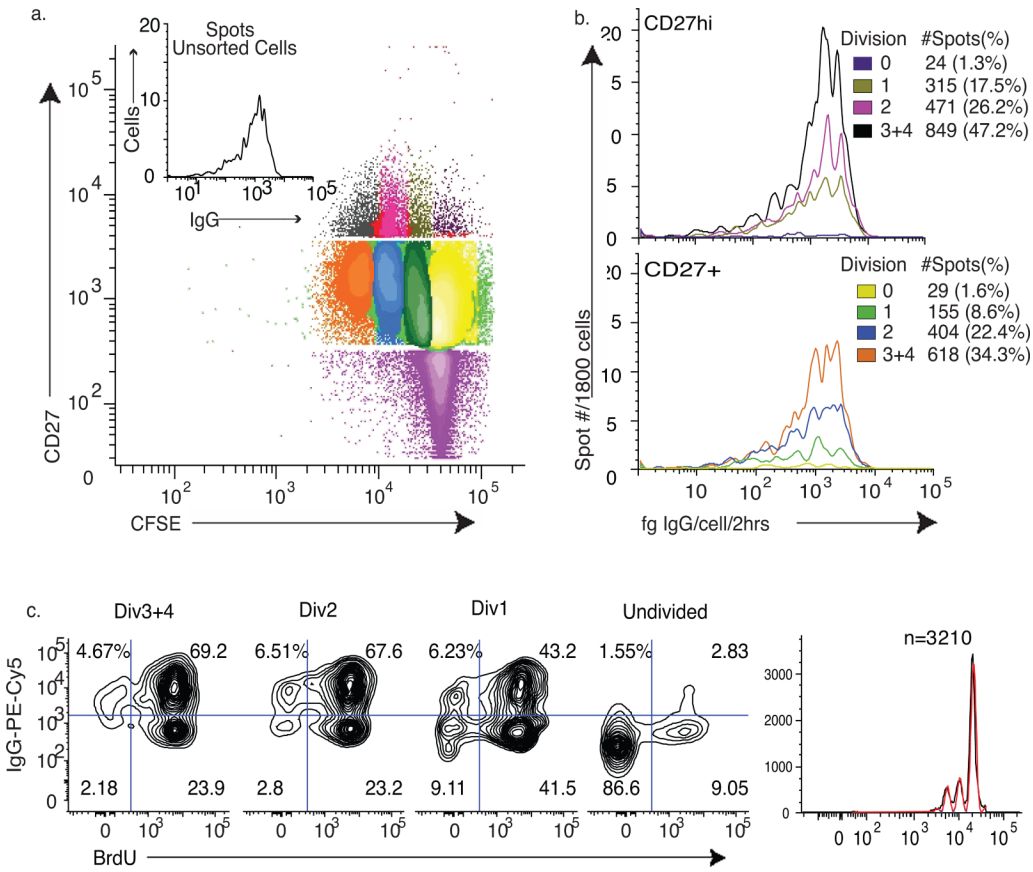

Figure 8. Binary On/Off IgG Secretion

IgM^{neg} Memory B cells were stained with CFSE, then stimulated with CpG+CK conditions for 72 hours. (a) IgG secretion of unsorted cells and gating figure for sorting. The cells were sorted first based on CD27 expression and then on CFSE content. The cells were counted and viability determined post-sort. (b) Of each fraction, 1800 live cells were plated in 6 wells at 300 cells/well for ELISPOT assay. Beads released IgG into other wells on each plate for standard curve generation. While the overall distribution of IgG secretion rates in each fraction remained the same, the frequency of IgG secreting cells and the preponderance of high-rate IgG-SC increased with division (N=4 experiments). Number of IgG-SC is shown as # spots (with % of cells plated) (c). IgM^{neg} memory B cells were stained with CFSE, incubated with BrdU under CpG+CK stimulation conditions for 69 hours. At harvest, the cells were fixed and stained for intracellular IgG and BrdU content. There are IgG positive and negative cells in each generation and the percent of IgG positive cells increases in each cell division, paralleling the increase in IgG secretion seen in Fig. 7. This suggests that not all cells produce IgG, even though they are dividing. Cells that remain undivided have a low percentage of IgG positive cells.